SI

A co-assembly process for a high strength and injectable dual network gel with sustained doxorubicin release performance

Chengcheng Zhao[1,2], Yanyao Wang[2], Lin Wang[3], Shuwen Lou[4], Bofang Shi [2], Yongfang Rao[*2], Mingtao Li[2], Wei Yan [2], Honghui Yang *[1]

1. Xi'an Key Laboratory of Sustainable Energy Materials Chemistry; School of Chemistry, Xi'an Jiaotong University, Xi'an 710049, China;
2. State Key Laboratory of Multiphase Flow in Power Engineering; Department of Environmental Science and Engineering, Xi'an Jiaotong University, Xi'an 710049, China;
3. First Affiliate Hospital of Xi'an Jiaotong University, Xi'an Jiaotong University, Xi'an 710049, China;
4. Hangzhou Entel Foreign Language School, Hangzhou 311122, China.

* Corresponding authors: yfrao@xjtu.edu.cn (Yongfang Rao); yanghonghui@mail.xjtu.edu.cn (Honghui Yang)

Table S1 The collected FTIR peak information of gels

Wavenumber / cm^{-1}	Vibration modes
3600	υ(-CONH-)
3317	υ (-COOH, H-bond)
3456	υ (-OH, -COOH, H-bond)
3063	υ(Aryl-H)
1725	υ (-COO-Fmoc, -CONH-(Amide I), -COOH)
1687	γ(-OH)
1633	$υ_{as}$ (G-COOH, M-COOH)
1610	β-sheet，$υ_{as}$ (-COO-)
1538	υ (Fmoc, Bz)
1450	γ(-CONH-) Amide II
1432	$υ_s$ (G-COOH, M-COOH)
1395	υ (-CONH-) Amide III
1256	υ(-OCO-Fmoc)
1080	υ(-CONH-)
1024	υ(-COOOC-)
740	β(Aryl-H)
563	β(-CH_2-)

Table S2 The collected data of ORCA calculation: the geometry optimization at B97-3C level, the single point energy at RI-B97M-V/def2-TZVP level and the binding energy (ΔE).

Conformation	Single point energy (SPE) / a.u.	ΔE / (kcal/mol)
Fmoc-F	-1282.960	\
ALG	-1446.194	\
DOX	-1928.674	\
Fmoc-F·Fmoc-F (1)	-2565.940	-12.613
Fmoc-F·Fmoc-F (2)	-2565.943	-14.478
Fmoc-F·H_2O·Fmoc-F	-2642.395	-28.964
Fmoc-F·2H_2O·Fmoc-F	-2718.842	-39.275
Fmoc-F·ALG (1)	-2729.175	-13.217
Fmoc-F·ALG (2)	-2729.198	-27.684
ALG·ALG	-2892.429	-25.777
ALG·Ca·ALG	-3570.168	-157.837
Fmoc-F·DOX (1)	-3211.668	-21.847
Fmoc-F·DOX (2)	-3211.669	-22.393
ALG·DOX (1)	-3374.919	-31.661
ALG·DOX (2)	-3374.906	-24.349
DOX·DOX (1)	-3857.393	-28.896
DOX·DOX (2)	-3857.384	-22.750
Fmoc-F·DOX·ALG (1)	-4657.909	-50.982
Fmoc-F·DOX·ALG (2)	-4657.912	-53.021

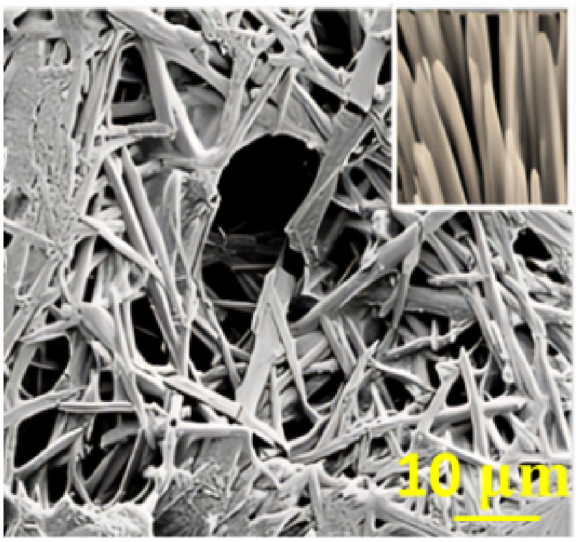

Figure S1 The network morphology overview of 1^{st}SN

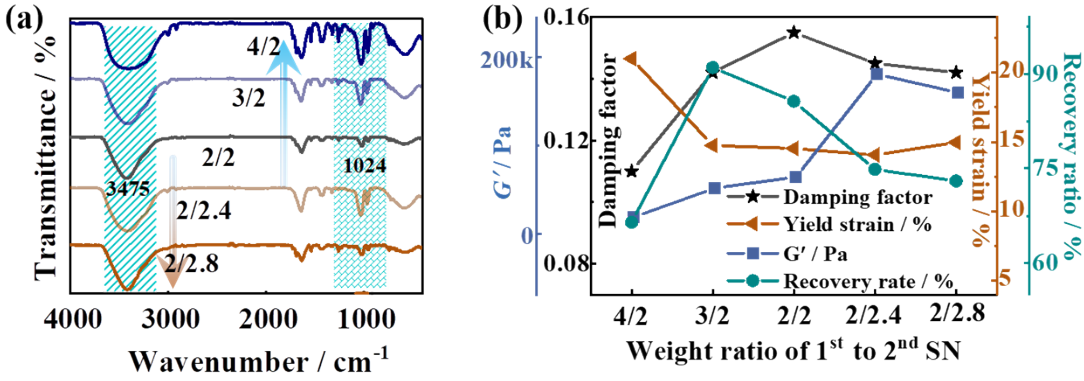

Figure S2 The dependency of DN gel properties on 1stSN/2ndSN ratio: (a) FTIR spectra and (b) rheological parameter's comparison.

Table S3 The collected rheological information of SN and DN gels.

The weight ratio of 1st SN to 2nd SN	Strain sweep				3ITT
	G' / Pa	G'' / Pa	Yield strain / %	$\tan\delta$	Recover ratio within 100 s / %
4/2	18700	2060	21.00	0.110	66.46
3/2	51700	7330	14.75	0.142	91.01
2/2	64400	9960	14.53	0.155	85.63
2/2.4	181000	26200	14.07	0.145	74.87
2/2.8	160000	22700	14.97	0.142	73.01

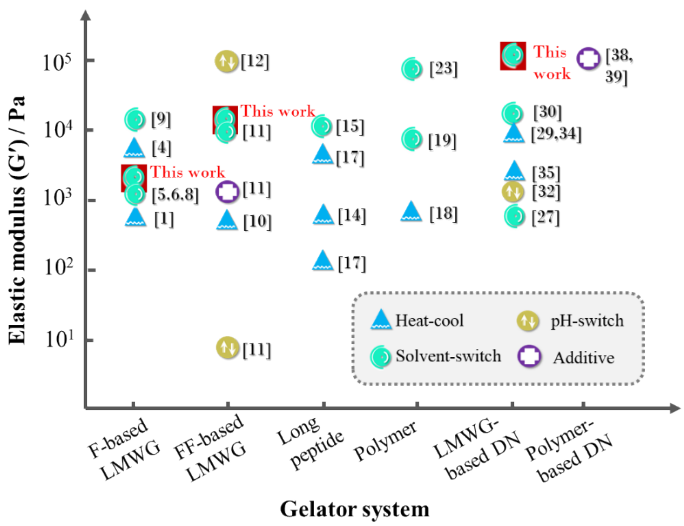

Figure S3 The comparison of elastic modulus of gels in this work and other types of gel materials.

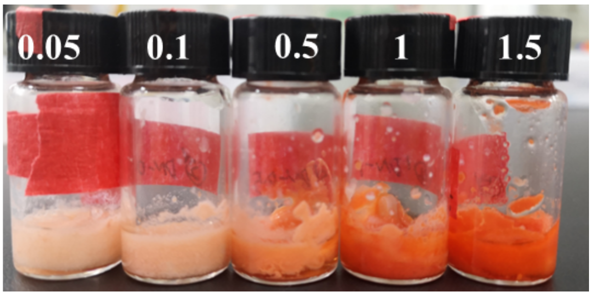

Figure S4 The optical pictures of DN-DOX-X gels with different DOX amounts (X=0.05, 0.1 0.5, 1 and 1.5).

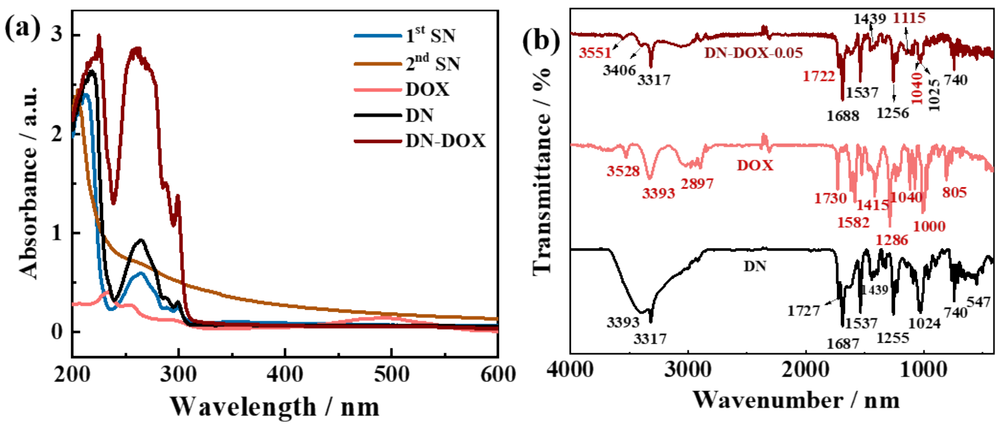

Figure S5 The structural change before and after DOX loading: (a) the UV-vis spectra, (b) FTIR spectra.

Table S4 The collecting rheological data of DN-DOX gels.

Sample	Strain sweep			3ITT
	G' / Pa	G'' /Pa	Yield strain / %	Recover ratio / %
DN-DOX-0.05	35600	6420	8.46	84.10
DN-DOX-0.1	57400	7190	14.29	89.60
DN-DOX-0.5	108000	13300	17.68	84.88
DN-DOX-1	60100	8350	16.88	88.53
DN-DOX-1.5	51800	8210	21.45	87.55

Table S5 The DOX loading efficiency, encapsulation efficiency and releasing in DN-DOX gels.

Drug delivery efficiency			1stSN-DOX-0.05	2ndSN-DOX-0.05	DN-DOX-x				
					0.05	0.1	0.5	1	1.5
Loading capacity	E_l / %		0.10	0.07	0.12	0.24	1.20	2.22	3.26
	E_e / %		77.06	59.11	96.71	95.48	97.47	90.65	89.77
Releasing profile	*Er at 30 min / %*		16.57	11.65	2.34	3.35	5.48	11.88	10.00
	E_r *at 24 h / %*		/	/	52.01	37.89	30.31	44.71	50.45
	t for E_r>50% / h		2	2	24	30	36	32	24
	t for E_r>90% / h		10	10	57	82	144	168	72
Fitting result of Er on a Rigter-Peppas model	Whole range	a	36.04	35.47	12.28	11.16	9.94	18.40	26.58
		n	**0.48**	**0.41**	**0.48**	**0.47**	**0.46**	**0.33**	**0.27**
		R^2	0.97	0.90	0.98	0.96	0.95	0.96	0.91
	0~24h	a_1	\		11.46	9.25	8.18	20.11	21.42
		n_1			**0.49**	**0.45**	**0.41**	**0.26**	**0.29**
		R_1^2			0.97	0.96	0.99	0.98	0.96
	24~48h	a_2			6.07	4.29	1.61	5.27	7.88
		n_2			**0.67**	**0.74**	**0.96**	**0.56**	**0.62**
		R_2^2			0.96	0.97	0.98	0.99	0.90
	48~End	a_3			42.60	34.19	23.34	38.25	69.58
		n_2			**0.19**	**0.22**	**0.28**	**0.17**	**0.06**
		R_3^2			0.72	0.82	0.97	0.88	0.84

Table S6 The release kinetics fitting by other models

Sample		Zero-order	First-order	Higuchi
1stSN-DOX-0.05		$y=20.63+9.26x$, $R^2=0.83$	$y=98.68\times(1-e^{-0.35x})$, $R^2=0.99$	$y=33.27\times x^{1/2}-0.03$, $R^2=0.97$
2ndSN-DOX-0.05		$y=26.51+1.09x$, $R^2=0.68$	$y=94.44\times(1-e^{-0.36x})$, $R^2=0.99$	$y=27.72\times x^{1/2}+4.16$, $R^2=0.89$
DN-DOX-x	0.05	$y=21.61+1.09x$, $R^2=0.87$	$y=103.09\times(1-e^{-0.03x})$, $R^2=0.97$	$y=11.33\times x^{1/2}+0.08$, $R^2=0.97$
	0.1	$y=24.20+0.77x$, $R^2=0.79$	$y=102.77\times(1-e^{-0.03x})$, $R^2=0.98$	$y=9.82\times x^{1/2}-0.05$, $R^2=0.95$
	0.5	$y=24.84+0.53x$, $R^2=0.77$	$y=98.36\times(1-e^{-0.02x})$, $R^2=0.98$	$y=8.10\times x^{1/2}+1.17$, $R^2=0.94$
	1	$y=35.65+0.44x$, $R^2=0.71$	$y=90.02\times(1-e^{-0.03x})$, $R^2=0.87$	$y=6.82\times x^{1/2}+15.17$, $R^2=0.92$
	1.5	$y=46.32+0.41x$, $R^2=0.52$	$y=90.91\times(1-e^{-0.05x})$, $R^2=0.91$	$y=7.04\times x^{1/2}+23.33$, $R^2=0.81$

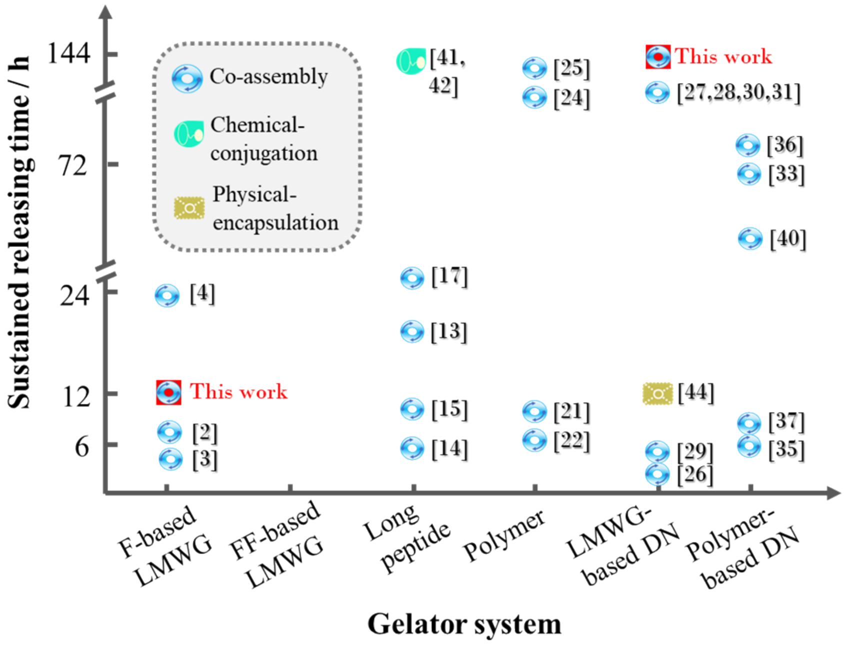

Figure S6 The comparison of sustained releasing time of gels in this work and other types of gel materials.

Reference:

[1] Murali DM, Shanmugam G. The aromaticity of the phenyl ring imparts thermal stability to a supramolecular hydrogel obtained from low molecular mass compound. New J Chem, 2019, 43 (31): 12396-12409.

[2] Gahane AY, Ranjan P, Singh V, et al. Fmoc-phenylalanine displays antibacterial activity against Gram-positive bacteria in gel and solution phases. Soft Matt, 2018, 14 (12): 2234-2244.

[3] Singh V, Snigdha K, Singh C, et al. Understanding the self-assembly of Fmoc-phenylalanine to hydrogel formation. Soft Matt, 2015, 11 (26): 5353-5364.

[4] Snigdha K, Singh BK, Mehta AS, et al. Self-assembling N -(9-Fluorenylmethoxycarbonyl)-l-Phenylalanine hydrogel as novel drug carrier. Int J Biol Macromol, 2016, 93: 1639-1646.

[5] Abraham JN, Joseph S, Trivedi R, et al. Injectable dextran-fluorenylmethoxycarbonyl phenylalanine composite hydrogels with improved mechanical properties. Polym Int, 2021, 70 (2): 222-229.

[6] Ryan DM, Anderson SB, Nilsson BL. The influence of side-chain halogenation on the self-assembly and hydrogelation of Fmoc-phenylalanine derivatives. Soft Matt, 2010, 6 (14): 3220.

[7] Ryan DM, Doran TM, Nilsson BL. Stabilizing self-assembled Fmoc-F5-Phe hydrogels by co-assembly with PEG-functionalized monomers. Chem Commun (Camb), 2011, 47 (1): 475-477.

[8] Hashemnejad SM, Huda MM, Rai N, et al. Molecular Insights into Gelation of Di-Fmoc-l-Lysine in Organic Solvent-Water Mixtures. ACS Omega, 2017, 2 (5): 1864-1874.

[9] Zhang Y, Li S, Ma M, et al. Tuning of gel morphology with supramolecular chirality amplification using a solvent strategy based on an Fmoc-amino acid building block. New J Chem, 2016, 40 (6): 5568-5576.

[10] Li J, Kuang Y, Shi J, et al. The conjugation of nonsteroidal anti-inflammatory drugs (NSAID) to small peptides for generating multifunctional supramolecular nanofibers/hydrogels. Beilstein J Org Chem, 2013, 9: 908-917.
[11] Raeburn J, Zamith Cardoso A, Adams DJ. The importance of the self-assembly process to control mechanical properties of low molecular weight hydrogels. Chem Soc Rev, 2013, 42 (12): 5143-5156.
[12] Najafi H, Abolmaali SS, Heidari R, et al. Nitric oxide releasing nanofibrous Fmoc-dipeptide hydrogels for amelioration of renal ischemia/reperfusion injury. J Control Release, 2021, 337: 1-13.
[13] Howe EJ, Okesola BO, Smith DK. Self-assembled sorbitol-derived supramolecular hydrogels for the controlled encapsulation and release of active pharmaceutical ingredients. Chem Commun (Camb), 2015, 51 (35): 7451-7454.
[14]Yu A, Hu Y, Ma X, et al. Sequential drug release of co-assembled supramolecular hydrogel as synergistic therapy against Staphylococcus aureus endophthalmitis. Chem Eng J, 2022, 427: 130979.
[15] Valls A, Isabel Burguete M, Kuret L, et al. Open chain pseudopeptides as hydrogelators with reversible and dynamic responsiveness to pH, temperature and sonication as vehicles for controlled drug delivery. J Mol Liq, 2021, 348: 118051.
[16] Dadfar SMR, Pourmahdian S, Tehranchi MM, et al. Novel dual-responsive semi-interpenetrating polymer network hydrogels for controlled release of anticancer drugs. J Biomed Mater Res A, 2019, 107 (10): 2327-2339.
[17] Tao N, Li G, Liu M, et al. Preparation of dual responsive low-molecular-weight hydrogel for long-lasting drug delivery. Tetrahedron, 2017, 73 (22): 3173-3180.
[18] Mo G, Zhang R, Wang Y, et al. Rheological and optical investigation of the gelation with and without phase separation in PAN/DMSO/H_2O ternary blends. Polymer, 2016, 84: 243-253.
[19] Appaw C, Gilbert RD, Khan SA, et al. Viscoelastic behavior of cellulose acetate in a mixed solvent system. Biomacromolecules, 2007, 8 (5): 1541-1547.
[20] Gonzalez MV, Tang Y, Phillips GJ, et al. Doxorubicin eluting beads-2: methods for evaluating drug elution and in-vitro:in-vivo correlation. J Mater Sci Mater Med, 2008, 19 (2): 767-775.
[21] Mao J, Qiu L, Ge L, et al. Overcoming multidrug resistance by intracellular drug release and inhibiting p-glycoprotein efflux in breast cancer. Biomed Pharmacother, 2021, 134: 111108.
[22] Maciel D, Figueira P, Xiao S, et al. Redox-responsive alginate nanogels with enhanced anticancer cytotoxicity. Biomacromolecules, 2013, 14 (9): 3140-3146.
[23] Ma M, Feng Z, Zhao M, et al. Fabrication of macrocyclic organogel utilizing solvent balance and its application in vascular supporting materials. Colloid Surf, 2020, 589: 124432.
[24] Zhou Q, Li C, Guo J, et al. Self-assembled biocompatible heparin-based supramolecular hydrogel for doxorubicin delivery. Carbohydr Res, 2022, 511: 108464.
[25] Wang M, Chen M, Niu W, et al. Injectable biodegradation-visual self-healing citrate hydrogel with high tissue penetration for microenvironment-responsive degradation and local tumor therapy. Biomaterials, 2020, 261: 120301.
[26] Dou XQ, Zhao CL, Mehwish N, et al. Photoresponsive supramolecular hydrogel co-assembled from Fmoc-Phe-OH and 4,4'-azopyridine for controllable dye release. Chinese J Polym Sci, 2019, 37 (5): 437-443.
[27] Chen J, Tao N, Fang S, et al. Incorporation of Fmoc-Y nanofibers into Ca-alginate hydrogels

for improving their mechanical properties and the controlled release of small molecules. New J Chem, 2018, 42 (12): 9651-9657.
[28] Shulman LP. Effectiveness of maternal influenza immunization in mothers and infants. yearbook of obstetrics, gynecology and women's health. N Engl J Med, 2009, 359: 115-117.
[29] Grijalvo S, Puras G, Zárate J, et al. Nioplexes encapsulated in supramolecular hybrid biohydrogels as versatile delivery platforms for nucleic acids. RSC Adv, 2016, 6 (46): 39688-39699.
[30] Huang R, Qi W, Feng L, et al. Self-assembling peptide–polysaccharide hybrid hydrogel as a potential carrier for drug delivery. Soft Matt, 2011, 7 (13): 6222.
[31] Gallo E, Diaferia C, Rosa E, et al. Peptide-based hydrogels and nanogels for delivery of doxorubicin. Int J Nanomedicine, 2021, 16: 1617-1630.
[32] Giuri D, Barbalinardo M, Zanna N, et al. Tuning mechanical properties of pseudopeptide supramolecular hydrogels by graphene doping. Molecules, 2019, 24 (23): 4345.
[33] Bai J, Liu Y, Jiang X. Multifunctional PEG-GO/CuS nanocomposites for near-infrared chemo-photothermal therapy. Biomaterials, 2014, 35 (22): 5805-5813.
[34] Piras CC, Mahon CS, Smith DK. Self-assembled supramolecular hybrid hydrogel beads loaded with silver nanoparticles for antimicrobial applications. Chem A Europ J, 2020, 26 (38): 8452-8457.
[35] Patterson AK, Smith DK. Two-component supramolecular hydrogel for controlled drug release. Chem Commun (Camb), 2020, 56 (75): 11046-11049.
[36] Vieira VMP, Hay LL, Smith DK. Multi-component hybrid hydrogels-understanding the extent of orthogonal assembly and its impact on controlled release. Chem Sci, 2017, 8 (10): 6981-6990.
[37] Nanda J, Biswas A, Banerjee A. Single amino acid based thixotropic hydrogel formation and pH-dependent morphological change of gel nanofibers. Soft Matt, 2013, 9 (16): 4198.
[38] Sun JY, Zhao X, Illeperuma WR, et al. Highly stretchable and tough hydrogels. Nature, 2012, 489 (7414): 133-136.
[39] Chen Q, Zhu L, Chen H, et al. A novel design strategy for fully physically linked double network hydrogels with tough, fatigue resistant, and self-healing properties. Adv Func Mater, 2015, 25 (10): 1598-1607.
[40] Zhang R, Xing R, Jiao T, et al. Carrier-free, chemophotodynamic dual nanodrugs via self-assembly for synergistic antitumor therapy. ACS Appl Mater Interfaces, 2016, 8 (21): 13262-13269.
[41] Zhao D, Zhao X, Zu Y, et al. Preparation, characterization, and in vitro targeted delivery of folate-decorated paclitaxel-loaded bovine serum albumin nanoparticles. Int J Nanomedicine, 2010, 5: 669-677.
[42] Yue Y, Liu ZW. Conjugating aldoxorubicin to supramolecular organic frameworks: polymeric prodrugs with enhanced therapeutic efficacy and safety. J Mater Chem B, 2022, 10(22): 4163-4171.
[43] Gao Y, Chen Y, Ji X, et al. Controlled intracellular release of Doxorubicin in multidrug-resistant cancer cells by tuning the shell-pore sizes of mesoporous silica nanoparticles. ACS Nano, 2011, 5 (12): 9788-9798.
[44] Ye W, Zhang G, Liu X, et al. Fabrication of polysaccharide-stabilized zein nanoparticles by flash nanoprecipitation for doxorubicin sustained release. 2022, 70: 103183.